Title: Acute accumulation of PIM2 and NRF2 and recovery of β5 subunit activity mitigate multiple myeloma cell susceptibility to proteasome inhibitors

Authors: Kimiko Sogabe[1], Shingen Nakamura[2], Yoshiki Higa[3], Hirokazu Miki[4], Asuka Oda[1], Tomoko Maruhashi[1], Ryohei Sumitani[1], Masahiro Oura[1], Mamiko Takahashi[1], Masafumi Nakamura[5], Yusaku Maeda[1], Tomoyo Hara[1], Hiroki Yamagami[1], Shiro Fujii[1], Kumiko Kagawa[6], Shuji Ozaki[6], Kiyoe Kurahashi[7], Itsuro Endo[8], Ken-ichi Aihara[2], Emiko Nakaue[3], Masahiro Hiasa[3], Jumpei Teramachi[9], Takeshi Harada[1], and Masahiro Abe[1,10]

Affiliations:

[1]Department of Hematology, Endocrinology and Metabolism, Tokushima University Graduate School of Biomedical Sciences, Tokushima, Japan

[2]Department of Community Medicine and Medical Science, Tokushima University Graduate School of Biomedical Sciences, Tokushima, Japan

[3]Department of Orthodontics and Dentofacial Orthopedics, Tokushima University Graduate School of Biomedical Sciences, Tokushima, Japan

[4]Division of Transfusion Medicine and Cell Therapy, Tokushima University Hospital, Tokushima, Japan

[5]Department of Internal Medicine, Tokushima Prefecture Naruto Hospital, Tokushima, Japan

[6]Department of Hematology, Tokushima Prefectural Central Hospital, Tokushima, Japan

[7]Department of Community Medicine for Respirology, Hematology and Metabolism, Tokushima University Graduate School of Biomedical Sciences, Tokushima, Japan

[8]Department of Bioregulatory Sciences, Tokushima University Graduate School of Biomedical Sciences, Tokushima, Japan

[9]Department of Oral Function and Anatomy, Graduate School of Medicine Dentistry and Pharmaceutical Sciences, Okayama University, Japan

[10]Department of Hematology, Kawashima Hospital, Tokushima, Japan

Running title: Mechanisms of myeloma cell resistance to proteasome inhibitors

Category: Original research

Word count: 5277

Figures 6; Tables 0; Supplementary Figures 3

References: 38

Correspondence:
Shingen Nakamura, Department of Community Medicine and Medical Science, Tokushima University Graduate School of Biomedical Sciences, Tokushima, Japan; 3-18-15 Kuramoto-cho, Tokushima, 770-8503, Japan
Tel.: +81-88-633-7120, FAX: +81-88-633-7121, e-mail: shingen@tokushima-u.ac.jp

Masahiro Abe, Department of Hematology, Kawashima Hospital, 6-1 Kitasakoichiban-cho, Tokushima, 770-0011, Japan. Tel.: +81-88-631-0110, Fax: +81-88-631-5500, e-mail: masabe@tokushima-u.ac.jp

Keywords: multiple myeloma, proteasome inhibitor, β5 subunit activity, PIM2, NRF2

Abstract

Resistance to proteasome inhibitors (PIs) has emerged as an important clinical issue. We investigated the mechanisms underlying multiple myeloma (MM) cell resistance to PIs. To mimic their pharmacokinetic/pharmacodynamic (PK/PD) profiles, MM cells were treated with bortezomib and carfilzomib for 1 hour at concentrations up to 400 and 1,000 nM, respectively. Susceptibility to these PIs markedly varied among MM cell lines. Pulsatile treatments with PIs suppressed translation, as demonstrated by incorporation of puromycin at 24 hours in PI-susceptible MM.1S cells, but not PI-resistant KMS-11 cells. Inhibition of β5 subunit activity decreased at 24 hours in KMS-11 cells, even with the irreversible PI carfilzomib, but not under suppression of protein synthesis with cycloheximide. Furthermore, the proteasome-degradable pro-survival factors PIM2 and NRF2 acutely accumulated in MM cells subjected to pulsatile PI treatments. Accumulated NRF2 was trans-localized into the nucleus to induce the expression of its target gene, *HMOX1*, in MM cells. PIM and Akt inhibition restored the anti-MM effects of PIs, even against PI-resistant KMS-11 cells. Collectively, these results suggest that increased synthesis of β5 proteasome subunit and acute accumulation of PIM2 and NRF2 reduce the anti-MM effects of PIs.

(187 words)

Introduction

The ubiquitin proteasome system (UPS) is a major target of treatment for multiple myeloma (MM), and proteasome inhibitors (PIs) are currently the therapeutic backbone for MM treatment. However, MM cell resistance to PIs has emerged as an insurmountable clinical issue. UPS degrades a wide variety of proteins, and, thus, the inhibition of proteasomal degradation may lead to the accumulation of proteins that are vital for MM cell growth and survival, which may, in turn, contribute to MM cell resistance to PIs. We previously reported that the serine/threonine kinase PIM2 was highly expressed in MM cells and played a critical role in their growth and survival [1, 2]. PIM2 was also found to be up-regulated in MM cells interacting with the bone marrow microenvironment and, thus, is regarded as an important therapeutic target. Consistent with previous findings showing the proteasomal degradation of the PIM2 protein [3], we demonstrated that a treatment with bortezomib (BTZ) and carfilzomib (CFZ) rapidly induced the accumulation of high PIM2 protein levels in MM cells to blunt the cytotoxic effects of PIs against MM cells [4]. The inhibition of PIM kinase enhanced the anti-MM effects of PIs. Therefore, the targeting of MM cell growth and survival factors that accumulate with the inhibition of proteasomes may augment the therapeutic efficacy of PIs.

The transcription factor (TF) nuclear factor erythroid 2-related factor 2 (NRF2) acts as a major cellular defense factor against oxidative stress and plays a critical role in cancer resistance to chemotherapeutic agents. NRF2 is also subject to proteasomal degradation. Under normal conditions, NRF2 binds to Kelch-like ECH-associated protein 1 (KEAP1), an adaptor protein of the cullin-RING ubiquitin ligase complex, to be ubiquitinated and rapidly degraded [5]. When oxidative stress is induced by external stress, such as anticancer agents, KEAP1 releases NRF2, which allows NRF2 to enter the nucleus [6]. The proteasomal degradation of NRF2 may also be mediated by glycogen synthase kinase (GSK)3β in a KEAP1-independent manner [7-9]. In cancer cells, the phosphatidylinositol 3-kinases (PI3K)/Akt pathway is activated to prevent the GSK3β-mediated degradation of NRF2 [10, 11]. When NRF2 localizes to the nucleus, it binds to an antioxidant response element as a heterodimer with a small Maf protein and initiates the transcription of antioxidant genes to protect cells from excessive reactive oxygen species (ROS) [12]. NRF2 systems mediate antioxidant defenses in cancer cells, and the up-regulation of NRF2 is widely accepted as an important mechanism of cancer cell resistance to anti-cancer agents.

The PK/PD profiles of PIs showed a high C_{max} with short $T_{1/2}$ in patients with MM treated with PIs. However, previous *in vitro* studies on PIs were mostly conducted with continuous exposure to low concentrations of PIs. To more accurately simulate the PK/PD

profiles of PIs, the effects of pulsatile treatments with PIs need to be examined. Therefore, we herein assessed the impact of pulsatile treatments with PIs at high concentrations on the viability of MM cells and their β5 subunit activity to elucidate the mechanisms underlying their resistance to PIs. The results obtained demonstrated that the recovery of β5 subunit activity and the robust accumulation of PIM2 and NRF2 proteins in MM cells after pulsatile treatments with PIs compromised the anti-MM effects of PIs, and also that the inhibition of PIM and Akt restored these effects.

Materials and Methods

Reagents

The following reagents were purchased from the indicated manufacturers: a rabbit anti-PIM2 antibody (Ab) (#4730), horseradish peroxidase (HRP)-conjugated goat anti-rabbit IgG Ab (#7074S), HRP-conjugated goat anti-mouse IgG Ab (#7076S), and BTZ from Cell Signaling Technology (Beverly, MA, USA); mouse anti-β-actin Ab (#A5451) and puromycin from Sigma-Aldrich (St Louis, MO, USA); anti-puromycin Ab (EQ0001) from Kerafast, Inc. (Boston, MA); SMI-16a from Calbiochem (Darmstadt, Germany); cycloheximide (CHX) from Nacalai Tesque (Kyoto, Japan), CFZ from ChemieTek (Indianapolis, IN, USA); rabbit anti-NRF2 Ab (#GTX103322) from Gene Tex (Los Angeles, USA); mouse anti-Nuclear matrix protein p84 Ab (#ab487) from Abcam (Cambridge, UK); and MK-2206 from Selleck Biotech (Tokyo, Japan). Phycoerythrin (PE)-labelled mouse monoclonal antibody against P-glycoprotein from Beckman Coulter Inc. (Brea, CA); PE-labelled mouse monoclonal antibody against breast cancer resistant protein (BCRP) and PE-labelled mouse IgG_1 from BioLegend (San Diego, CA); mouse monoclonal antibody against multidrug resistance-associated protein 1 (MRP1) (#sc-53130) from SantaCruz Biotechnology (Dallas, TX); Mouse IgG1 for control was from Agilent (Santa Clara, CA); and Fluorescein Isothiocyanate (FITC) -labelled Goat anti-Mouse IgG Secondary Antibody from Thermo Fisher Scientific Inc. (Waltham, MA).

Cells

The human MM cell lines, RPMI 8226, MM.1S, U266, and H929 were obtained from the American Type Culture Collection (Manassas, VA). The OPM-2 cell line was purchased from the German Collection of Microorganisms and Cell Cultures (Braunschweig, Germany). The KMS-11 cell line was obtained from the Japanese Collection of Research Bioresources Cell Bank (Osaka, Japan). Cells were cultured in RPMI 1640 medium (Sigma-Aldrich) supplemented with 5% fetal bovine serum (Thermo Fisher Scientific, Waltham MA, USA), 100 U/mL penicillin (Sigma-Aldrich), and 100 μg/mL streptomycin

(Sigma-Aldrich).

Peripheral blood mononuclear cells (PBMCs) were collected from normal donor samples as previously described [13]. Mononuclear cells were separated from peripheral blood or bone marrow aspirates using Ficoll-Paque PLUS (GE Healthcare Bio-Sciences AB, Uppsala, Sweden). Primary CD138-positive cells were purified using anti-CD138 magnetic activated cell separation microbeads (Miltenyi Biotec, San Diego, CA) from mononuclear cells isolated from the bone marrow aspirates of patients with MM. The collection of human samples was conducted under written informed consent according to the Declaration of Helsinki and the protocols of the Institutional Review Board (3842 in Tokushima University Hospital and 16-8 in Tokushima Prefectural Central Hospital).

Cell viability and ATP quantification assays

Cell viability and ATP quantification were performed using Cell Counting Kit-8 (CCK-8) (Dojindo Laboratories, Kumamoto, Japan) and the Cell Titer-Glo assay, respectively.

Proteasome β5 subunit activity assays

Proteasome β5 subunit activity was analyzed as described in a previous study [14]. In brief, MM cells were washed twice using ice-cold phosphate-buffered saline (PBS) and centrifuged for 5 min. Cell pellets were resuspended in proteolysis buffer (50 mM Tris HCl, 25 mM KCl, 10 mM NaCl, 1 mM $MgCl_2$, and 0.1 mM 1,4-dithiothreitol (DTT)) and subjected to a 5-min freeze/5-min thaw cycle 3 times using dry ice and a water bath. Samples were then centrifuged at 13,000 rpm for 10 min to pellet debris and the supernatant was collected for protein quantification. Protein concentrations were assessed by the BCA assay (Bio-Rad). Three micrograms of protein from samples were loaded into 96-well black plates containing proteolysis buffer and 20 μM 7-amino-4-methylcoumarin (AMC) substrate to a final volume of 100 μL per well. The AMC substrate Suc-LLVY-AMC (Enzo Life Sciences, Farmingdale, NY, USA) was used to measure chymotrypsin-like activity exhibited by the β5 subunit. Fluorescence was measured using the SpectraMax i3 microplate reader (Molecular Device, Tokyo, Japan) at excitation and emission wavelengths of 355 and 444 nm, respectively. Each sample was run in triplicate.

Western blot analysis

Whole cell lysates were lysed in radioimmunoprecipitation buffer with protease inhibitor cocktail solution (Sigma-Aldrich), phosphatase inhibitor (FUJIFILM Wako Pure Chemical Corporation), 1 mmol/l phenylmethylsulfonyl fluoride (FUJIFILM Wako Pure Chemical Corporation), and DTT (FUJIFILM Wako Pure Chemical Corporation).

Nuclear proteins were extracted using the NE-PER^{NT} nuclear and cytoplasmic extraction reagent kit (Thermo Fisher Scientific, Rockford, IL, USA). Protein concentrations were measured using the Pierce^{TM} BCA Protein Assay Kit (Bio-Rad). Mixtures of cell lysates and 3ME-sample buffer (FUJIFILM Wako Pure Chemical Corporation) were heated at 95℃ for 5 min. Samples were electrophoresed on 5-20% gradient gels and transferred to polyvinylidene difluoride membranes (Bio-Rad). After blocking with 3% bovine serum albumin (FUJIFILM Wako Chemicals Corporation) or 3% non-fat dry milk in tris–buffered saline with 0.01% Tween 20 (TBS-T), membranes were incubated with primary antibodies at 4℃ overnight, followed by HRP-conjugated secondary Abs for 1 hour. Protein bands were visualized using Immobilon Forte Western HRP substrates (Millipore, MA, USA).

Plasmids

NFE2L2 pLKO.1 short hairpin RNA (shRNA) vectors were purchased from Sigma-Aldrich. The target sequences of the respective vectors were as follows: #1; AGTTTGGGAGGAGCTATTATC (TRCN0000273494) and #2; AGAGCAAGATTTAGATCATTT (TRCN0000281950). A luciferase pLKO.1 shRNA vector (shLuc) was used as a negative control of transduction. To induce human *NFE2L2* complementary DNA (cDNA) in MM cells, a plasmid pHAGE-*NFE2L2*, which was kindly provided by Gordon B. Mills (Addgene plasmid #116765), was used.

Quantitative real-time PCR (qRT-PCR) analysis

RNAs were extracted from cells using TRI REAGENT (Molecular Research Center, Cincinnati, Ohio). cDNAs were synthesized from RNAs extracted using the PrimeScript RT Master Mix (Takara Bio Inc., Shiga, Japan). qRT-PCR was performed using a Quant Studio 3 Real-Time PCR System (Thermo Fisher Scientific) with the following temperature protocol: at 95°C for 10 min, followed by 40 cycles at 95°C for 30 sec and 60°C for 1 min. In qRT-PCR, each cDNA sample was mixed with 10 μL SYBR® qPCR mixα (NIPPON GENE CO., LTD, Japan), a forward (Fwd) primer, reverse (Rev) primer, template cDNA, and nuclease-free water. The total volume was 20 μL/reaction. The following primers were used:

GAPDH; Fwd: TGTCTTCACCACCATGGAGAAGG, Rev: GTGGATGCAGGGATGATGTTCTG, *NFE2L2*; Fwd: GTTGCCCACATTCCCAAATC, Rev: TGACTGAAACGTAGCCGAAGAA,

PSMB5 Fwd: TGCTTGCCAACATGGTGTATC, Rev: TGAAATCCGGTTCCCTTCAC,

PIM2; Fwd: CCATTCCCGTGGAGTTGT, Rev: GAAGCAGGGCACCAGAAC

HMOX1; Fwd: AGTGCCACCAAGTTCAAGCA, Rev: CAGCTCCTGCAACTCCTCAA, and, *PPIE*; Fwd: TGGACGTACAATTCGTGTCAA, Rev: GGCTCTGACCCTTCTTCCTC.

Transduction

Lentiviral production was performed as previously described [15]. In brief, pLKO.1-based plasmids or the pHAGE-*NFE2L2* plasmid were transfected into 293T cells in combination with pCMV-dvpr and VSV-G for lentiviral packaging using TransIT-LT1 Transfection Reagent (Mirus Bio, Madison, WI). Virus-containing media were then harvested according to previous methods [15]. MM cells were cultured with virus-containing media in the presence of polybrene (Santa-Cruz) for 5 hours. After 24 hours, shRNA-induced MM cells were selected using 1 μg/mL puromycin (Sigma-Aldrich) for 48 hours. cDNA-induced MM cells, which expressed EGFP, were sorted by flow cytometry. The selected cells were used in subsequent experiments.

Flow cytometry

Cells were incubated with PBS containing 1% BSA and stained with PE-labelled antibodies or isotype control for 30 minutes on ice. For detection of MRP expression, cells were incubated with primary antibody or IgG as above. After washing, the cells were washed and resuspended with an FITC-labeled secondary antibody for 30 minutes on ice. After washing, the cells were analyzed with CytoFLEX (BECKMAN COULTER, CA). Data were edited using FlowJo software (BD Biosciences San Jose, CA).

Statistical analysis

Statistical analyses were performed with EZR (Saitama Medical Center, Jichi Medical University, Saitama, Japan). Data distributions were analyzed using the Shapiro-Wilk test. The significance of differences was evaluated using the Student's *t*-test for two normally distributed groups and the Tukey-Kramer multiple comparison test for multiple normally distributed groups. The Mann-Whitney U test was used for the two non-normally distributed groups and the Steel-Dwass test for multiple non-normally distributed groups. $P < 0.05$ was considered to be significant.

Results

Cytotoxic activities of pulsatile PI treatments vary among MM cell lines

In terms of the experimental conditions for exposure to BTZ or CFZ, we followed a previous study with experiments modeling the anticipated *in vivo* pharmacokinetics of

drug exposure in patients with MM [17]. We set experimental conditions with a 1-hour pulsatile treatment with BTZ or CFZ at concentrations between 50 and 400 and between 125 and 1,000 nM, respectively. Continuous treatments with BTZ and CFZ at more than 50 nM were effective against all the MM cell lines tested (Fig. S1). However, while BTZ and CFZ dose-dependently induced cell death in MM.1S and U266 cells at concentrations between 50 and 400 and between 125 and 1,000 nM, respectively, KMS-11, OPM-2, and RPMI8226 cells were resistant to the exposure to BTZ at these concentrations and CFZ at 125 nM (Fig. 1A). KMS-11 cells were the most resistant against these PIs among the MM cell lines tested, whereas MM.1S cells were the most susceptible. Consistently, the production of ATP was reduced more in MM.1S cells than in OPM-2 and KMS-11 cells by the pulsatile treatment with CFZ (Fig. 1B). Excessive endoplasmic reticulum (ER) stress induced by PIs is considered to be an essential mechanism for the induction of the anti-MM effects of PIs, in which eIF2α is phosphorylated to trigger the global inhibition of protein translation in cells [18]. Therefore, we investigated protein translation after the pulsatile treatment with PIs. Puromycin is an analog of the 3' end of aminoacyl-tRNA, which may be incorporated into translated nascent proteins [19]. The incorporation of puromycin was assessed after a 1-hour pulsatile treatment with CFZ. Puromycin incorporation was reduced in MM.1S cells and slightly in OPM-2 cells, but not in KMS-11 cells 12 and 24 hours after the pulsatile treatment with CFZ (Fig. 1C), suggesting a relationship between the suppression of translation in MM cells and the cytotoxic effects of CFZ.

Basal β5 subunit activity and durability of its inhibition after pulsatile PI treatments

Since the susceptibilities of the MM cell lines to a pulsatile treatment with BTZ or CFZ markedly varied (Fig. 1A), we examined the baseline enzymatic activity of a β5 subunit of the proteasome, a major target of BTZ and CFZ, in MM cells. KMS-11 cells exhibited the highest catalytic activity of the β5 subunit, and the susceptibilities of the respective MM cell lines to these PIs were inversely associated with their β5 subunit activity levels at the baseline (Fig. 2A). We also investigated the time course of β5 subunit activity in MM cells after the treatment with BTZ or CFZ. MM.1S cells were susceptible to pulsatile treatments for 1 hour with BTZ and CFZ at 50 and 100 nM, while KMS-11 cells were completely resistant to these concentrations (Fig. 1A). β5 subunit activity was immediately suppressed and at 9 hours after the pulsatile treatment in KMS-11, MM1.S and OPM-2 cell lines. However, β5 subunit activity mostly recovered after 24 hours in PI-resistant KMS-11 (Fig. 2B) and OPM-2 cells (Fig. S2A), but remained low in MM.1S cells (Fig. 2B) treated with BTZ at 100 nM and CFZ at 50 and 100 nM. We then examined

the recovery of β5 subunit activity in KMS-11 cells subjected to the pulsatile treatment for 1 hour with higher concentrations of these PIs. KMS-11 cells were insensitive to the pulsatile treatment with BTZ up to 400 nM, but were partially susceptible to CFZ at 500 and 1,000 nM (Fig. 1A). At 24 hours, β5 subunit activity in KMS-11 cells was almost completely restored to control levels upon the treatment with BTZ at 400 nM and partially with CFZ at 400 and 1,000 nM (Fig. S2B). These results suggest that baseline levels and the durability of the inhibition of β5 subunit activity in MM cells correlated with the cytotoxic activity of PIs.

Since CFZ is an irreversible inhibitor of a β5 proteasome subunit, we assumed that a newly synthesized β5 proteasome subunit may contribute to the recovery of proteasomal activity from immediate suppression in PI-resistant KMS-11 cells after the pulsatile CFZ treatment. Therefore, we investigated the recovery of β5 subunit activity 24 hours after the pulsatile treatment with CFZ in the presence or absence of CHX, an inhibitor of protein synthesis at the translational level. Under the suppression of protein synthesis with CHX, β5 subunit activity did not recover and remained low in KMS-11 cells 24 hours after the pulsatile treatment with CFZ (Fig. 2C), indicating that protein synthesis was required for the recovery of β5 subunit activity after the PI treatment. Collectively, these results suggest that strong basal β5 subunit activity and the robust production of a β5 subunit compromised MM cell susceptibility to PIs.

Immediate accumulation of PIM2 and NRF2 proteins in MM cells after the PI treatments

Similar to the findings of our previous study on the effects of continuous treatments with BTZ and CFZ [4], the pulsatile treatment with BTZ or CFZ induced the accumulation of the PIM2 protein in MM cells (Fig. 3A). The up-regulation of the ROS reliever NRF2 is one of the major protective mechanisms in cancer cells against anti-cancer cytotoxic agents. NRF2 is rapidly degraded by proteasomes [20]. In the present study, NRF2 accumulated in parallel with PIM2 in MM cells after pulsatile PI treatments (Fig. 3A). Although the pulsatile treatment with CFZ markedly increased PIM2 and NRF2 protein levels, these changes were mostly abolished under the suppression of protein synthesis with CHX (Fig. 3B). However, the pulsatile PI treatment reduced *PIM2* expression and slightly increased *NFE2L2* (*NRF2*) expression in MM cells at the mRNA level (Fig. 3C). These results suggest that PIM2 and NRF2 were robustly produced in MM cells to a sufficient amount to overcome their rapid proteasomal degradation, and also that these proteins markedly accumulated in MM cells after proteasomal inhibition.

NRF2 is a critical pro-survival mediator in MM cells

When NRF2 evades its proteasomal degradation, it localizes to the nucleus and up-regulates the transcription of its target antioxidant genes, such as the heme oxygenase-1 gene (*HMOX1*), to protect cells from excessive oxidative stress [12]. The present results revealed the marked accumulation of NRF2 in MM cells subjected to the pulsatile PI treatments (Fig. 3A, B). We then examined the nuclear localization of NRF2 and its target *HMOX1* gene expression in MM cells following the pulsatile PI treatments. The nuclear localization of NRF2 was observed in MM.1S, OPM-2 and KMS-11 cells immediately and 3 hours after the pulsatile PI treatments for 1 hour (Fig. 4A), and this was followed by the induction of *HMOX1* gene expression (Fig. 4B). The knockdown of *NFE2L2* markedly reduced the cell viability of KMS-11 cells (Fig. 4C), indicating that NRF2 functions as a vital survival factor. Conversely, its overexpression compromised the cytotoxicity of PIs against MM cells (Fig. 4D). These results suggest that the PI treatments induced the accumulation of NRF2 to compromise PI-induced cell death in MM cells.

PIM and Akt inhibition potentiate anti-MM effects of PIs

We previously reported that the inhibition of PIM enhanced the anti-MM effects of PIs, while PIs induced the accumulation of PIM2 in MM cells [4]. Akt activation in cancer cells has been shown to suppress the β-transducin repeat containing protein (β-TrCP)-mediated proteasomal degradation of NRF2. Therefore, we investigated the effects of the inhibition of PIM and Akt in combination with the pulsatile PI treatment. The PIM inhibitor SMI-16a and Akt inhibitor MK-2206 cooperatively reduced the cell viability of KMS-11 and OPM-2 cells (Fig. 5A) and primary MM cells (Fig. S3) in the absence of PIs. The inhibition of PIM and Akt also potentiated the cytotoxic effects of BTZ and CFZ against MM cells. Although KMS-11 and OPM-2 cells were resistant to the pulsatile treatment with BTZ at the concentrations up to 400 nM and CFZ at 100 and 250 nM (Fig. 1A), the PIM and Akt inhibitors in combination with PIs induced cytotoxic effects on these cells. The pulsatile treatment with CFZ at 250 nM markedly increased NRF2 protein levels along with the expression of *HMOX1*, its target gene (Fig. 5B); however, the Akt inhibitor MK-2206 added after CFZ reduced NRF2 and *HMOX1* levels. MK-2206 alone reduced NRF2 levels in MM.1S and OPM-2 cells, upon the pulsatile treatment with CFZ (Fig. 5C), indicating the role of Akt in increasing NRF2 protein levels in MM cells. These results suggest that the inhibition of PIM and Akt restored and potentiated the anti-MM effects of PIs.

Expression of ATP-binding cassette (ABC) transporters on MM cells.

Because the upregulation of ABC transporters can cause drug resistance, we analyzed the expression of ABC transporters, P-glycoprotein, breast cancer resistant protein (BCRP) and multidrug resistance-associated protein 1 (MRP1) in RPMI8226, OPM-2 and KMS-11 cells. P-glycoprotein and MRP1 were marginally expressed in RPMI8226, OPM-2 and KMS-11 cells (Fig. 6). BCRP was expressed in RPMI8226 and KMS-11 cells. The expression of these ABC transporters was not apparently affected after the pulsatile treatment with CFZ.

Discussion

Proteasomes control the equilibrium between protein synthesis and degradation, and maintain cellular function and survival. The proteasome load versus capacity balance affects the apoptotic sensitivity of MM cells to PIs [21]. Consistent with this notion, β5 proteasome subunit activity was higher in PI-resistant KMS-11 cells than in PI-sensitive MM.1S cells. The mechanisms underlying the up-regulation of proteasome β5 subunit production and activity in MM cells are suggested to be multifaceted [22-24] and include NRF1/2 activation [25-28]; however, they remain largely unknown. Furthermore, β5 activity recovered more in PI-resistant KMS-11 cells than in PI-sensitive MM.1S cells, even with the irreversible PI CFZ. However, the blockade of translation by CHX suppressed the recovery of β5 activity after the CFZ treatment. Therefore, the production of large amounts of the β5 proteasome subunit may restore β5 subunit activity, even following a treatment with the irreversible inhibitor CFZ, and thereby compromise the cytotoxic effects of PIs against MM cells. These results suggest that the capacity of β5 subunit production and the recovery of β5 subunit activity confer the resistance of MM cells to PIs.

Proteasome inhibition results in the accumulation of misfolded and functional proteins in the lumen of the ER and cytosol, thereby leading to ER overload, ROS overproduction, functional intracellular protein disorders, and apoptosis in MM cells [29-31]. However, PIs block the degradation of a wide variety of proteins, including those favoring MM cell growth and survival, thereby contributing to drug resistance in MM. We previously identified the anti-apoptotic mediator PIM2 as an example of this [1, 2, 4]. In addition to PIM2, we showed the marked accumulation of NRF2, a master TF for redox homeostasis, following the pulsatile treatment. NRF2 activation in cancer cells promotes disease progression [32-34] and metastasis [35], and also confers resistance to chemo- and radiotherapies [36, 37]. Accumulated NRF2 was promptly trans-localized to the nucleus (Fig. 4A) in order to induce the transcription of its target antioxidant gene,

HMOX1 (Fig. 4B). The knockdown of *NFE2L2* alone reduced cell viability in KMS-11 cells (Fig. 4C), suggesting an important role of NRF2 in cell survival. Hypoxia is considered to be among major causes of the drug resistance in MM cells. The NRF2-HMOX1 axis has been reported to contribute to hypoxia-induced resistance to PIs in vitro and in vivo [38]. Given the increase of NRF protein levels in MM cells under hypoxic condition [38], the pulsatile treatment of PIs is suggested to more robustly increase NRF2 in MM cells under hypoxic condition, which further contribute to the resistance of MM cells to PIs. These results indicate that PIM2 and NRF2 are robustly synthesized and subjected to β5 subunit-mediated degradation in MM cells, and also that treatments with PIs induce the accumulation of PIM2 and NRF2 to mitigate their anti-MM effects.

The PI3K/Akt pathway is aberrantly activated in many cancers. NRF2 was previously shown to be activated by the PI3K/Akt pathway in order for cancer cells to acquire resistance to chemotherapeutic agents [33, 34]. GSK3β binds to the SKP1-CUL1-RBX1 E3 ubiquitin ligase complex and ubiquitylates NRF2. The activation of the PI3K/Akt pathway inhibits GSK3β, thereby allowing NRF2 to be degraded by β-TrCP-mediated proteasomal degradation [7, 8]. Akt inhibition has been shown to enhance NRF2 degradation in cancer cells by relieving GSK3β from its phosphorylation-mediated repression. In the present study, the inhibition of Akt reduced NRF2 levels in MM cells (Fig. 5B, C). In addition, PIM2 and phosphorylated Akt cooperatively activate mTORC1, which initiates translation. The addition of the PIM inhibitor SMI-16a and the Akt inhibitor MK-2206 after pulsatile treatments with PIs cooperatively enhanced anti-MM effects, even against PI-resistant MM cells (Fig. 5A). These results provide a rationale for novel combinations of PIs with PIM and Akt inhibitors to overcome MM cell resistance to PIs. The mechanisms underlying the recovery of β5 activity after PI treatments warrant further study with special reference to NRF2-mediated stress adaptation.

Acknowledgments

This work was supported by JSPS KAKENHI Grant Numbers JP22K08455, JP21H0311, JP22K19626, JP17H05104, JP19K22719, and JP23H03101; the Research Clusters program of Tokushima University (2202003, T.H.); and the Japanese Society of Hematology Research Grants (T.H. and H.M). The funders had no role in the study design, data collection and analysis, decision to publish, or preparation of the manuscript.

Conflict of Interest

T.H. received research funding from GlaxoSmithKline. M.A. received research funding

from Chugai Pharmaceutical, Sanofi K.K., Pfizer Seiyaku K.K., Kyowa Hakko Kirin, Janssen Pharma K.K., Takeda Pharmaceutical, Teijin Pharma, and Ono Pharmaceutical, and honoraria from Daiichi Sankyo Company. The other authors declare no competing financial interests.

Authors' Contributions

KS, SN, TH, and MA contributed to the study design. KS, YH, OA, and TM conducted experiments. SN, HM, RS, MO, MT, MN, YM, SF, KK, SO, and TH contributed to the collection of clinical samples. TH, HY, KK, IE, KA, EN, MH, and TJ reviewed data. KS, SN, TH, and MA wrote and revised the manuscript. All authors were involved in the analyses and interpretation of data. All authors read and approved the submitted version of the manuscript.

References

1. Asano J, Nakano A, Oda A, Amou H, Hiasa M, Takeuchi K et al. The serine/threonine kinase Pim-2 is a novel anti-apoptotic mediator in myeloma cells. Leukemia. 2011;25(7):1182-8. doi:10.1038/leu.2011.60.

2. Hiasa M, Teramachi J, Oda A, Amachi R, Harada T, Nakamura S et al. Pim-2 kinase is an important target of treatment for tumor progression and bone loss in myeloma. Leukemia. 2015;29(1):207-17. doi:10.1038/leu.2014.147.

3. Adam K, Lambert M, Lestang E, Champenois G, Dusanter-Fourt I, Tamburini J et al. Control of Pim2 kinase stability and expression in transformed human haematopoietic cells. Bioscience reports. 2015;35(6). doi:10.1042/bsr20150217.

4. Fujii S, Nakamura S, Oda A, Miki H, Tenshin H, Teramachi J et al. Unique anti-myeloma activity by thiazolidine-2,4-dione compounds with Pim inhibiting activity. Br J Haematol. 2018;180(2):246-58. doi:10.1111/bjh.15033.

5. Itoh K, Wakabayashi N, Katoh Y, Ishii T, Igarashi K, Engel JD et al. Keap1 represses nuclear activation of antioxidant responsive elements by Nrf2 through binding to the amino-terminal Neh2 domain. Genes & development. 1999;13(1):76-86. doi:10.1101/gad.13.1.76.

6. Kobayashi A, Kang MI, Watai Y, Tong KI, Shibata T, Uchida K et al. Oxidative and electrophilic stresses activate Nrf2 through inhibition of ubiquitination activity of Keap1. Mol Cell Biol. 2006;26(1):221-9. doi:10.1128/mcb.26.1.221-229.2006.

7. Rada P, Rojo AI, Chowdhry S, McMahon M, Hayes JD, Cuadrado A. SCF/{beta}-TrCP promotes glycogen synthase kinase 3-dependent degradation of the Nrf2 transcription factor in a Keap1-independent manner. Mol Cell Biol. 2011;31(6):1121-33.

doi:10.1128/mcb.01204-10.
8. Rada P, Rojo AI, Evrard-Todeschi N, Innamorato NG, Cotte A, Jaworski T et al. Structural and functional characterization of Nrf2 degradation by the glycogen synthase kinase 3/β-TrCP axis. Mol Cell Biol. 2012;32(17):3486-99. doi:10.1128/mcb.00180-12.
9. Chowdhry S, Zhang Y, McMahon M, Sutherland C, Cuadrado A, Hayes JD. Nrf2 is controlled by two distinct β-TrCP recognition motifs in its Neh6 domain, one of which can be modulated by GSK-3 activity. Oncogene. 2013;32(32):3765-81. doi:10.1038/onc.2012.388.
10. Rojo AI, Medina-Campos ON, Rada P, Zúñiga-Toalá A, López-Gazcón A, Espada S et al. Signaling pathways activated by the phytochemical nordihydroguaiaretic acid contribute to a Keap1-independent regulation of Nrf2 stability: Role of glycogen synthase kinase-3. Free radical biology & medicine. 2012;52(2):473-87. doi:10.1016/j.freeradbiomed.2011.11.003.
11. Yu C, Xiao JH. The Keap1-Nrf2 System: A Mediator between Oxidative Stress and Aging. Oxidative medicine and cellular longevity. 2021;2021:6635460. doi:10.1155/2021/6635460.
12. Itoh K, Chiba T, Takahashi S, Ishii T, Igarashi K, Katoh Y et al. An Nrf2/small Maf heterodimer mediates the induction of phase II detoxifying enzyme genes through antioxidant response elements. Biochem Biophys Res Commun. 1997;236(2):313-22. doi:10.1006/bbrc.1997.6943.
13. Abe M, Hiura K, Wilde J, Shioyasono A, Moriyama K, Hashimoto T et al. Osteoclasts enhance myeloma cell growth and survival via cell-cell contact: a vicious cycle between bone destruction and myeloma expansion. Blood. 2004;104(8):2484-91. doi:10.1182/blood-2003-11-3839.
14. Bonet-Costa V, Sun PY, Davies KJA. Measuring redox effects on the activities of intracellular proteases such as the 20S Proteasome and the Immuno-Proteasome with fluorogenic peptides. Free radical biology & medicine. 2019;143:16-24. doi:10.1016/j.freeradbiomed.2019.07.020.
15. Harada T, Ohguchi H, Oda A, Nakao M, Teramachi J, Hiasa M et al. Novel antimyeloma therapeutic option with inhibition of the HDAC1-IRF4 axis and PIM kinase. Blood advances. 2023;7(6):1019-32. doi:10.1182/bloodadvances.2022007155.
16. Kitazoe KI, Abe M, Hiasa M, Oda A, Amou H, Harada T et al. Valproic acid exerts anti-tumor as well as anti-angiogenic effects on myeloma. Int J Hematol. 2009;89(1):45-57. doi:10.1007/s12185-008-0226-9.
17. Kuhn DJ, Chen Q, Voorhees PM, Strader JS, Shenk KD, Sun CM et al. Potent activity of carfilzomib, a novel, irreversible inhibitor of the ubiquitin-proteasome pathway,

against preclinical models of multiple myeloma. Blood. 2007;110(9):3281-90. doi:10.1182/blood-2007-01-065888.
18. Ameri K, Harris AL. Activating transcription factor 4. The international journal of biochemistry & cell biology. 2008;40(1):14-21. doi:10.1016/j.biocel.2007.01.020.
19. Goodman CA, Pierre P, Hornberger TA. Imaging of protein synthesis with puromycin. Proc Natl Acad Sci U S A. 2012;109(17):E989; author reply E90. doi:10.1073/pnas.1202000109.
20. Baird L, Yamamoto M. The Molecular Mechanisms Regulating the KEAP1-NRF2 Pathway. Mol Cell Biol. 2020;40(13). doi:10.1128/mcb.00099-20.
21. Bianchi G, Oliva L, Cascio P, Pengo N, Fontana F, Cerruti F et al. The proteasome load versus capacity balance determines apoptotic sensitivity of multiple myeloma cells to proteasome inhibition. Blood. 2009;113(13):3040-9. doi:10.1182/blood-2008-08-172734.
22. Oerlemans R, Franke NE, Assaraf YG, Cloos J, van Zantwijk I, Berkers CR et al. Molecular basis of bortezomib resistance: proteasome subunit beta5 (PSMB5) gene mutation and overexpression of PSMB5 protein. Blood. 2008;112(6):2489-99. doi:10.1182/blood-2007-08-104950.
23. Lü S, Wang J. The resistance mechanisms of proteasome inhibitor bortezomib. Biomarker research. 2013;1(1):13. doi:10.1186/2050-7771-1-13.
24. Shirazi F, Jones RJ, Singh RK, Zou J, Kuiatse I, Berkova Z et al. Activating KRAS, NRAS, and BRAF mutants enhance proteasome capacity and reduce endoplasmic reticulum stress in multiple myeloma. Proc Natl Acad Sci U S A. 2020;117(33):20004-14. doi:10.1073/pnas.2005052117.
25. Li B, Fu J, Chen P, Ge X, Li Y, Kuiatse I et al. The Nuclear Factor (Erythroid-derived 2)-like 2 and Proteasome Maturation Protein Axis Mediate Bortezomib Resistance in Multiple Myeloma. J Biol Chem. 2015;290(50):29854-68. doi:10.1074/jbc.M115.664953.
26. Chen T, Ho M, Briere J, Moscvin M, Czarnecki PG, Anderson KC et al. Multiple myeloma cells depend on the DDI2/NRF1-mediated proteasome stress response for survival. Blood advances. 2022;6(2):429-40. doi:10.1182/bloodadvances.2020003820.
27. Op M, Ribeiro ST, Chavarria C, De Gassart A, Zaffalon L, Martinon F. The aspartyl protease DDI2 drives adaptation to proteasome inhibition in multiple myeloma. Cell death & disease. 2022;13(5):475. doi:10.1038/s41419-022-04925-3.
28. Sun Y, Abdul Aziz A, Bowles K, Rushworth S. High NRF2 expression controls endoplasmic reticulum stress induced apoptosis in multiple myeloma. Cancer Lett. 2018;412:37-45. doi:10.1016/j.canlet.2017.10.005.
29. Adams J. The proteasome: a suitable antineoplastic target. Nat Rev Cancer.

2004;4(5):349-60. doi:10.1038/nrc1361.
30. Pérez-Galán P, Roué G, Villamor N, Montserrat E, Campo E, Colomer D. The proteasome inhibitor bortezomib induces apoptosis in mantle-cell lymphoma through generation of ROS and Noxa activation independent of p53 status. Blood. 2006;107(1):257-64. doi:10.1182/blood-2005-05-2091.
31. Fink EE, Mannava S, Bagati A, Bianchi-Smiraglia A, Nair JR, Moparthy K et al. Mitochondrial thioredoxin reductase regulates major cytotoxicity pathways of proteasome inhibitors in multiple myeloma cells. Leukemia. 2016;30(1):104-11. doi:10.1038/leu.2015.190.
32. DeNicola GM, Karreth FA, Humpton TJ, Gopinathan A, Wei C, Frese K et al. Oncogene-induced Nrf2 transcription promotes ROS detoxification and tumorigenesis. Nature. 2011;475(7354):106-9. doi:10.1038/nature10189.
33. Satoh H, Moriguchi T, Takai J, Ebina M, Yamamoto M. Nrf2 prevents initiation but accelerates progression through the Kras signaling pathway during lung carcinogenesis. Cancer Res. 2013;73(13):4158-68. doi:10.1158/0008-5472.Can-12-4499.
34. Tao S, Liu P, Luo G, Rojo de la Vega M, Chen H, Wu T et al. p97 Negatively Regulates NRF2 by Extracting Ubiquitylated NRF2 from the KEAP1-CUL3 E3 Complex. Mol Cell Biol. 2017;37(8). doi:10.1128/mcb.00660-16.
35. Wang H, Liu X, Long M, Huang Y, Zhang L, Zhang R et al. NRF2 activation by antioxidant antidiabetic agents accelerates tumor metastasis. Science translational medicine. 2016;8(334):334ra51. doi:10.1126/scitranslmed.aad6095.
36. Padmanabhan B, Tong KI, Ohta T, Nakamura Y, Scharlock M, Ohtsuji M et al. Structural basis for defects of Keap1 activity provoked by its point mutations in lung cancer. Mol Cell. 2006;21(5):689-700. doi:10.1016/j.molcel.2006.01.013.
37. Singh A, Misra V, Thimmulappa RK, Lee H, Ames S, Hoque MO et al. Dysfunctional KEAP1-NRF2 interaction in non-small-cell lung cancer. PLoS Med. 2006;3(10):e420. doi:10.1371/journal.pmed.0030420.
38. Abe K, Ikeda S, Nara M, Kitadate A, Tagawa H, Takahashi N. Hypoxia-induced oxidative stress promotes therapy resistance via upregulation of heme oxygenase-1 in multiple myeloma. Cancer medicine. 2023;12(8):9709-22. doi:10.1002/cam4.5679.

Figure legends

Figure 1. Cytotoxic activities of pulsatile treatments with PIs vary among MM cell lines. (A - C) MM cell lines were treated with bortezomib (BTZ) or carfilzomib (CFZ) at the indicated concentrations for 1 hour. Cells were washed with PBS twice and then subjected to each assay. Cell viability was assessed using (A) CCK-8 and (B) Cell Titer-Glo 24 hours after the pulsatile treatment. (A, B) Results represent relative changes from the baseline (100%) with the mean ± SD (n = 3). ***P < .001 significantly different between MM.1S and KMS-11 cells under 100 and 1000 nM CFZ-treated conditions; the Tukey-Kramer multiple comparison test. (C) After incubating treated cells for 0, 12, or 24 hours, cells were then exposed to puromycin for 15 minutes. The whole cell lysates extracted were subjected to Western blotting in order to detect the incorporation of puromycin. β-actin served as a loading control.

Figure 2. Durability of the inhibition of β5 subunit activity in MM cells after the pulsatile treatments with PIs. (A - C) Cell lysates were extracted from the indicated MM cell lines and peripheral blood mononuclear cells (PBMCs), followed by the β5 subunit activity assay as described in the Materials and Methods. (B) KMS-11 and MM.1S cells were treated with BTZ or CFZ at the indicated concentrations for 1 hour. Cells were washed with PBS twice and then subjected to the assay at 0, 9, and 24 hours. Data are shown as relative changes from the baseline (100%) of PI-naïve KMS-11 cells at each time point. (C) KMS-11 cells were treated with CFZ at 50 or 250 nM for 1 hour. Cells washed with PBS twice were cultured for 24 hours in the presence or absence of cycloheximide (CHX), followed by the β5 subunit activity assay. Relative changes from the baseline (100%) are shown. Data represent mean ± SD (n = 3).

Figure 3. **Immediate accumulation of PIM2 and NRF2 in MM cells after pulsatile treatments with PIs.** (A - C) MM.1S, OPM-2, and KMS-11 cells were treated with (A) BTZ or CFZ, (A - C) CFZ at the indicated concentrations for 1 hour. After washing cells with PBS twice, cells were cultured for 6 hours (B) in the presence or absence of CHX. (A, B) The lysates extracted were subjected to Western blotting. β-actin served as the loading control. (C) Total RNAs extracted were subjected to quantitative real-time PCR (qRT-PCR). *GAPDH* served as an endogenous control to normalize each sample. Relative changes from the baseline are shown. Data represent the mean ± SD (n = 3).

Figure 4. **NRF2 is a critical pro-survival mediator in MM cells.** (A) MM.1S , KMS-11 and OPM-2 cells were treated with or without 200 nM BTZ or 500 nM CFZ for 1 hour.

Treated cells were washed with PBS twice, followed by the extraction of nuclear and cytoplasmic proteins immediately (0 hour) and 3 hours after the pulsatile treatment. The lysates extracted were subjected to Western blotting. p84 and GAPDH served as loading controls for nucleic and cytoplasmic lysates, respectively. (B) MM.1S, KMS-11 and OPM-2 cells were treated with or without CFZ at 50 and 250 nM for 1 hour, respectively. Treated cells were washed with PBS twice, followed by the extraction of total RNAs before (Pre) and after the pulsatile treatment at the indicated time points. Total RNAs extracted were subjected to qRT-PCR. *PPIE* served as an endogenous control to normalize each sample. Relative changes from the baseline are shown. (C) KMS-11 cells were transduced with either sh*NFE2L2* (#1 and #2) or sh*Luc* as a control. After puromycin selection for 48 hours, cell viability for 24 hours was assessed using CCK-8 and the whole cell lysates extracted were subjected to Western blotting. (D) RPMI 8226 cells were transduced with *NFE2L2* cDNA or Empty. After GFP-positive selection by flow cytometry, cells were treated with or without BTZ or CFZ at the indicated concentrations for 1 hour. Cells washed with PBS twice were cultured for 24 hours and then subjected to the CCK-8 assay. The whole cell lysates extracted were subjected to Western blotting. β-actin served as a loading control. % changes from the baseline are shown. Data represent the means ± SD (n = 3). ***P < .001 significantly different between the groups; (B, C) the Tukey-Kramer multiple comparison test and (C) Student's *t*-test. ns; not significant.

Figure 5. **PIM and Akt kinase inhibition potentiates anti-MM effects of PIs.** (A, B) KMS-11 and OPM-2 cells were treated with or without BTZ (100 nM) or CFZ (250 nM) for 1 hour. After washing cells twice with PBS, they were treated with or without SMI-16a (50 μM), MK-2206 (5 μM), or their combination for 48 hours and then subjected to (A) the CCK-8 assay. % changes from the baseline of the non-treatment condition are shown. Data represent means ± SD (n = 3). (B) Whole cell lysates and total RNAs were extracted from the treated cells at 12 hours, followed by Western blotting and qRT-PCR. β-actin served as a loading control for Western blotting. *PPIE* served as an endogenous control to normalize each sample in qRT-PCR. Relative changes from the baseline are shown. Data represent the means ± SD (n = 3). ***P < .001 significantly different between the groups; the Tukey-Kramer multiple comparison test. (C) MM.1S and OPM-2 cells were cultured in the presence or absence of CFZ at 50 and 250 nM for 1 hour, respectively. After washing cells twice with PBS, MM.1S cells were treated with 2.5 μM MK-2206 for 20 hours. OPM-2 cells were treated with 5 μM MK-2206 for 24 hours. The whole cell lysates extracted were subjected to Western blotting. β-actin served as a loading control.

Figure 6. Expression of ATP-binding cassette (ABC) transporters on MM cells.
RPMI8226, OPM-2 and KMS-11 cells were incubated with or without CFZ at the indicated concentrations for 1 hour. The expression of P-glycoprotein (P-GP), breast cancer resistant protein (BCRP) and multidrug resistance-associated protein 1 (MRP1) was analyzed followed by the flowcytometry at 24 hours. The background is shown in gray shadow.

Figure

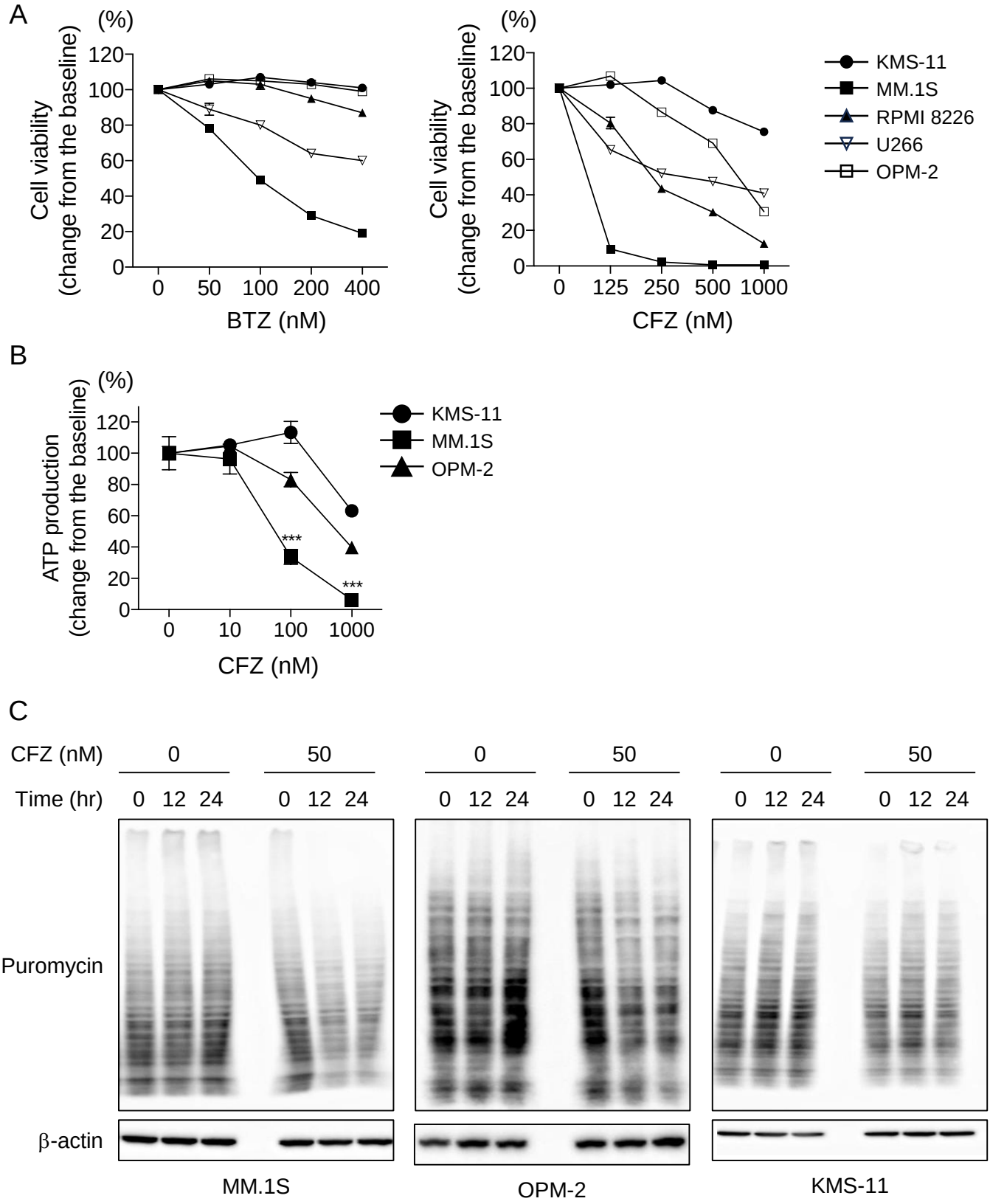

Figure 1

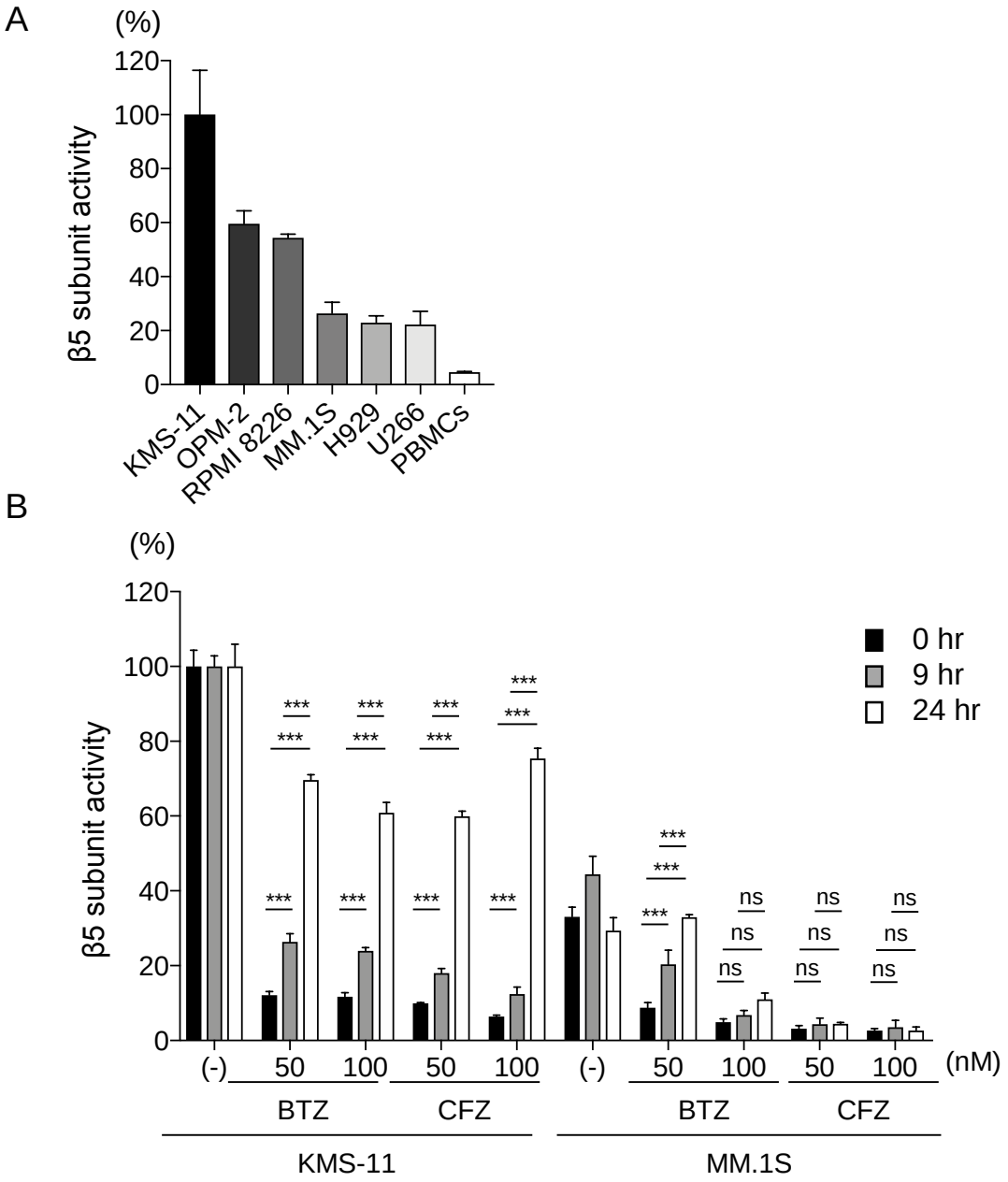
A
(%)
120
100
80
60
40
20
0
β5 subunit activity
KMS-11
OPM-2
RPMI 8226
MM.1S
H929
U266
PBMCs
B
(%)
120
100
80
60
40
20
0
β5 subunit activity
0 hr
9 hr
24 hr
***
ns
(-)
50
100
(nM)
BTZ
CFZ
KMS-11
MM.1S
C
(%)
CHX
(-)
(+)
β5 subunit activity
(-)
50
250
CFZ (nM)

Figure 2

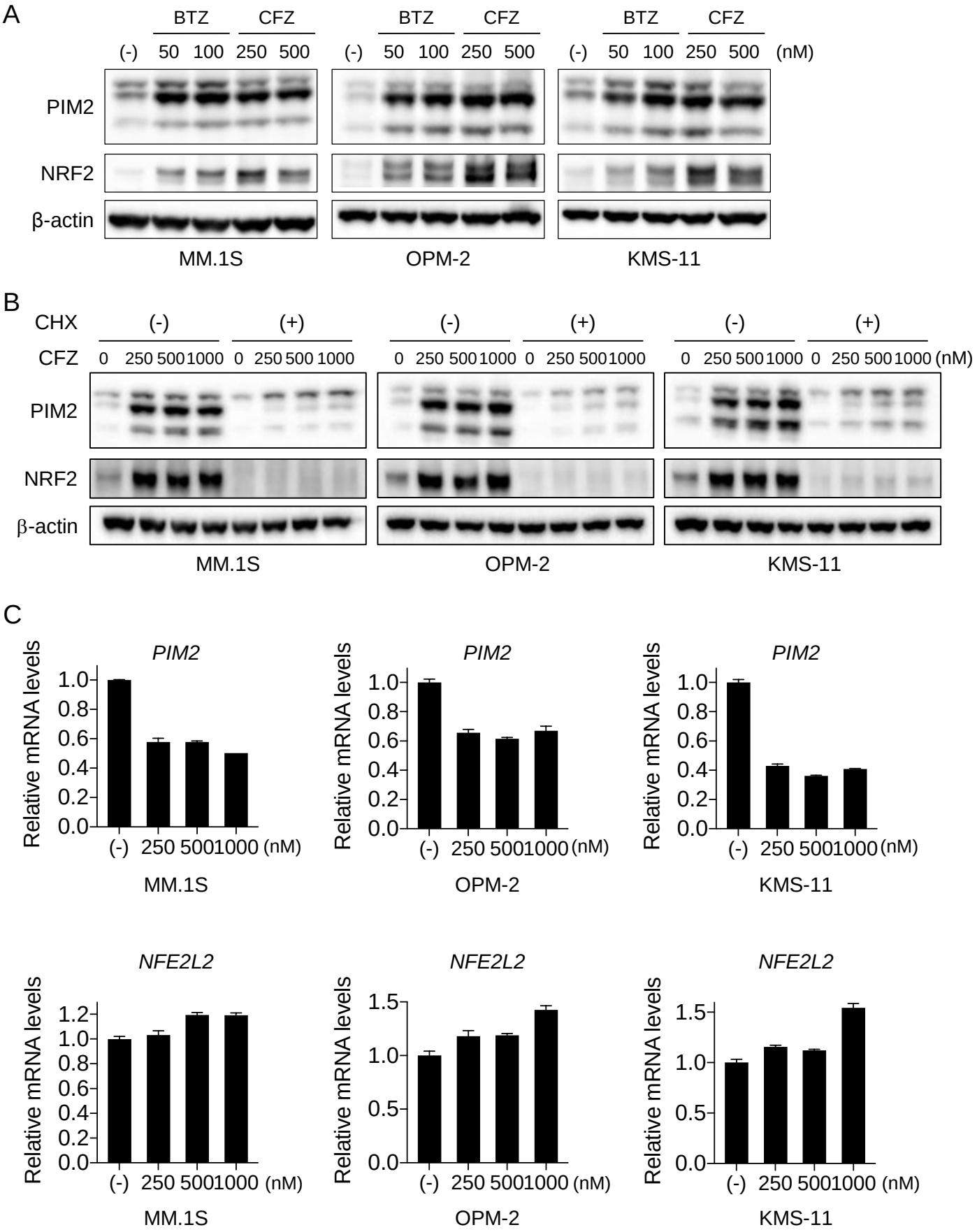
A
BTZ
CFZ
(-) 50 100 250 500 (nM)
PIM2
NRF2
β-actin
MM.1S
OPM-2
KMS-11
B
CHX
(-)
(+)
CFZ
0 250 500 1000 (nM)
PIM2
NRF2
β-actin
MM.1S
OPM-2
KMS-11
C
PIM2
NFE2L2
Relative mRNA levels
(-) 250 500 1000 (nM)
MM.1S
OPM-2
KMS-11

Figure 3

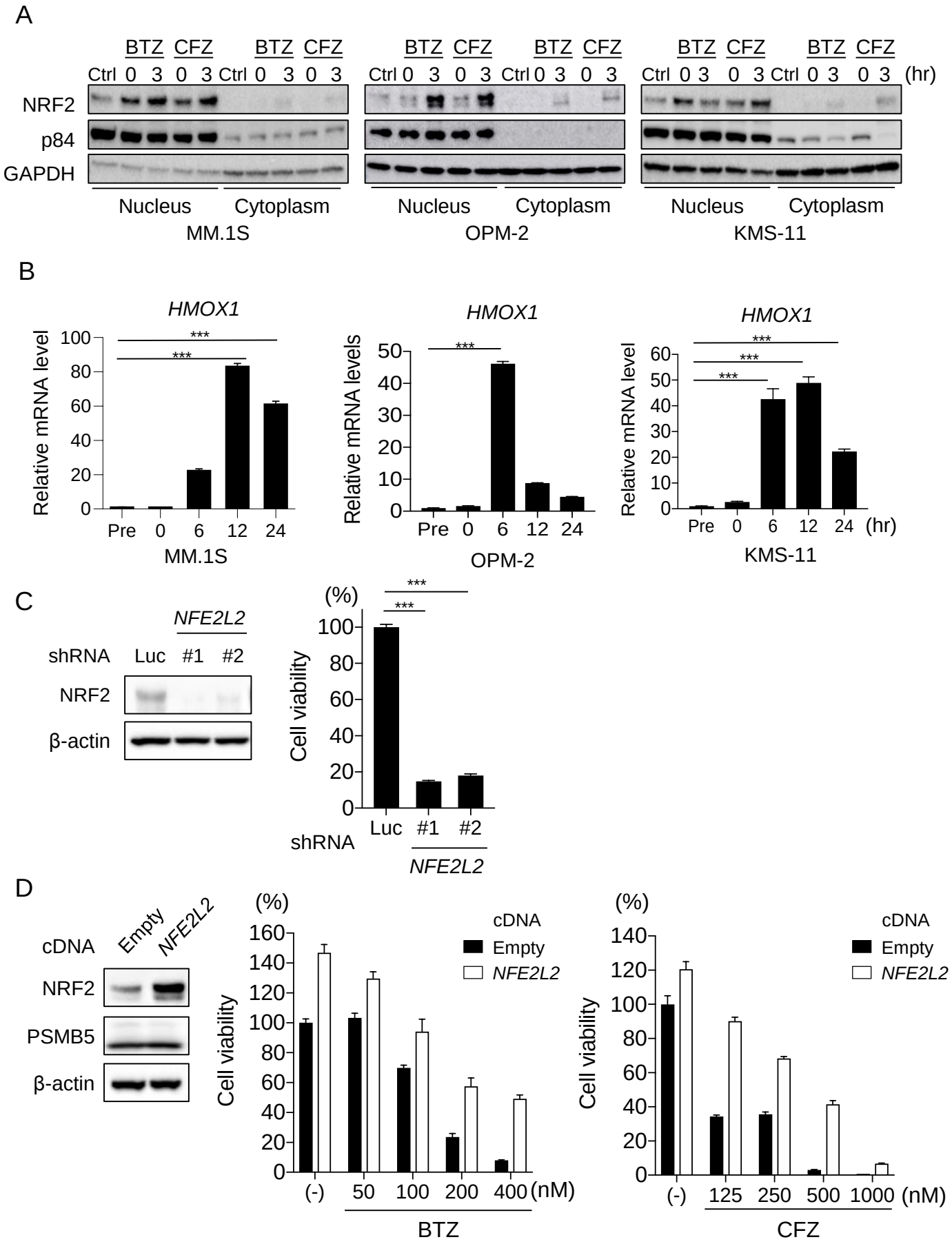
A
BTZ CFZ BTZ CFZ
Ctrl 0 3 0 3 Ctrl 0 3 0 3
(hr)
NRF2
p84
GAPDH
Nucleus Cytoplasm
MM.1S
OPM-2
KMS-11
B
HMOX1
Relative mRNA level
Relative mRNA levels
***
Pre 0 6 12 24 (hr)
MM.1S
OPM-2
KMS-11
C
NFE2L2
shRNA Luc #1 #2
NRF2
β-actin
(%)
Cell viability
Luc #1 #2
shRNA
NFE2L2
D
cDNA Empty NFE2L2
NRF2
PSMB5
β-actin
(%)
Cell viability
cDNA
Empty
NFE2L2
(-) 50 100 200 400 (nM)
BTZ
(-) 125 250 500 1000 (nM)
CFZ

Figure 4

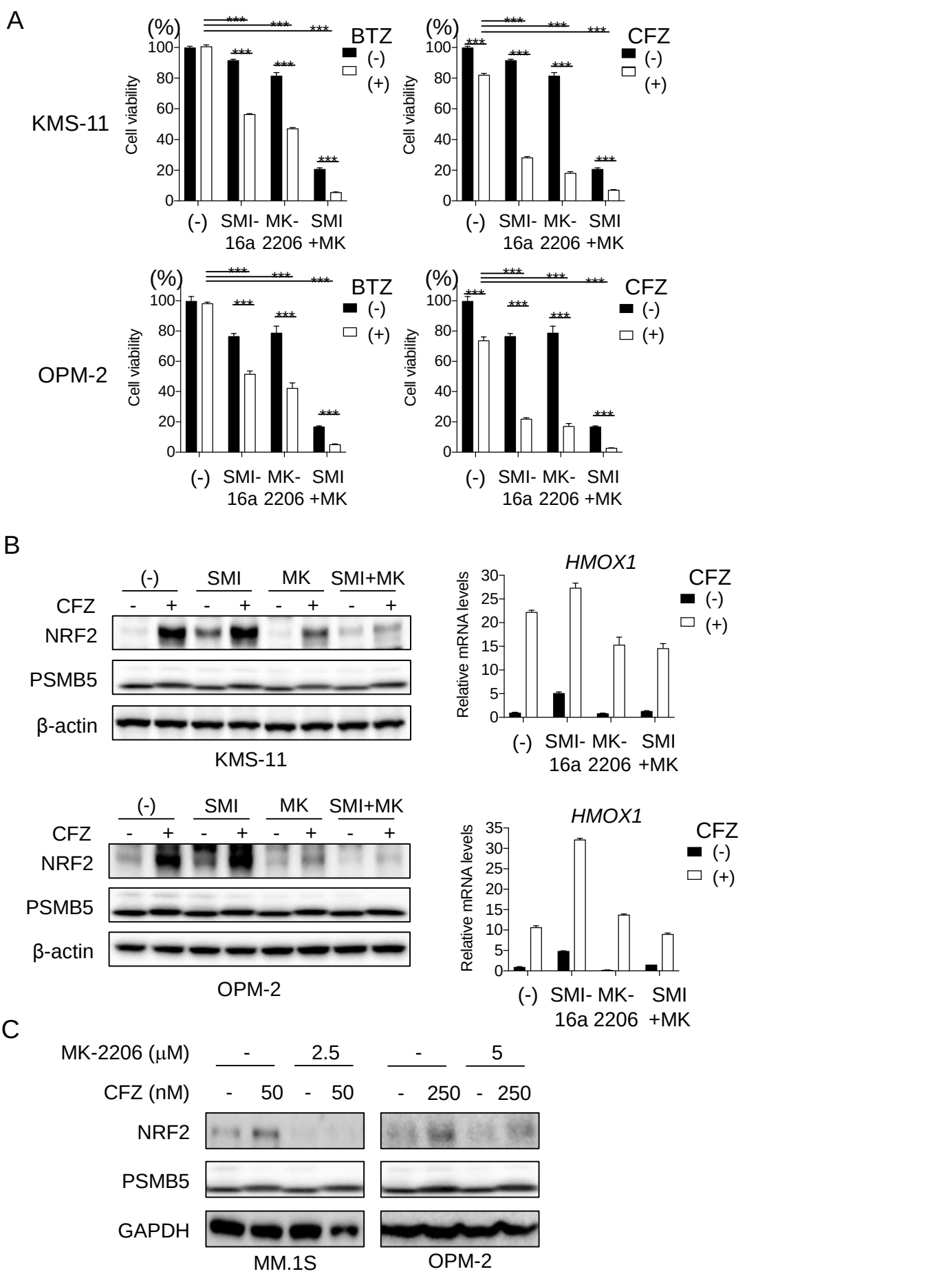
A
KMS-11
OPM-2
BTZ
CFZ
(%)
Cell viability
(-)
(+)
(-)
SMI-16a
MK-2206
SMI +MK
B
(-)
SMI
MK
SMI+MK
CFZ
NRF2
PSMB5
β-actin
KMS-11
OPM-2
HMOX1
Relative mRNA levels
C
MK-2206 (μM)
CFZ (nM)
GAPDH
MM.1S
OPM-2

Figure 5

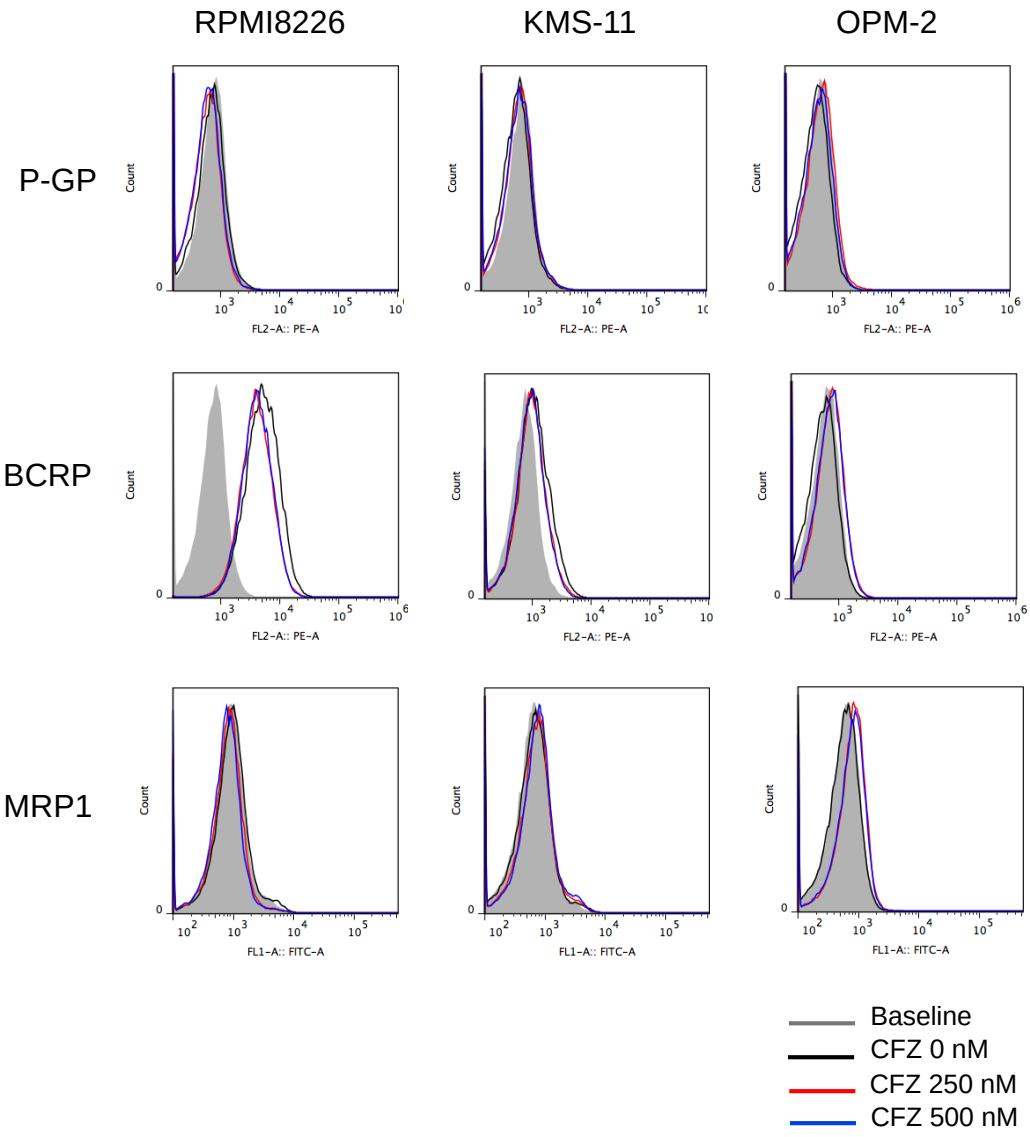
RPMI8226
KMS-11
OPM-2
P-GP
BCRP
MRP1
Count
FL2-A:: PE-A
FL1-A:: FITC-A
Baseline
CFZ 0 nM
CFZ 250 nM
CFZ 500 nM

Figure 6